

## A NOVEL HETEROSTRUCTURED CdS/AgFeO<sub>2</sub> NANOCOMPOSITE AS AN EFFICIENT VISIBLE-LIGHT PHOTOCATALYST FOR THE DEGRADATION OF CONGO RED

Z. SONG\*, F. WANG, Y.Q. HE, P. LIN, S.W. LIN

*College of Chemistry, Changchun Normal University, Changchun 130032, Jilin, People's Republic of China*

The novel CdS/AgFeO<sub>2</sub> nanocomposites were synthesized via a two-step chemical process including the hydrothermal and the chemical bath deposition methods. The as-synthesized photocatalysts were characterized by X-ray powder diffraction (XRD), scanning electron microscopy (SEM), and PL spectra (PL) techniques. The photocatalytic degradation of Congo Red (CR) was investigated in detail. The results revealed that the modification of CdS could efficiently improve the photocatalytic activity of the AgFeO<sub>2</sub> photocatalyst. Additionally, the quenching investigation of different scavengers demonstrated that h<sup>+</sup>, •OH, •O<sub>2</sub><sup>-</sup> reactive species played different roles in the decolorization of CR. Our results showed that CdS/AgFeO<sub>2</sub> nanocomposites could be used as an effective photocatalyst.

(Received April 16, 2018; Accepted August 10, 2018)

**Keywords:** Heterostructured, CdS/AgFeO<sub>2</sub>, Degradation efficiency

### 1. Introduction

Photocatalysis, a promising strategy for the degradation of dyes and organic pollutants of wastewater, can offer a clean and renewable technology to convert them into less organic matters such as CO<sub>2</sub> and H<sub>2</sub>O by utilizing the solar light [1-6]. Ag-based material with delafossite oxide AgMO<sub>2</sub> (M=Fe, Co, Ni, Cr) have attracted much attention owing to their excellent electronic structure [7,8]. Especial, AgFeO<sub>2</sub> has been considered as an excellent photocatalytic activity due to its narrow bandgap and high activity, and the theory calculation indicate its band gap energy was narrow enough for AgFeO<sub>2</sub> to generate electrons and holes under visible light irradiation. However, the photocatalytic activity of the pure AgFeO<sub>2</sub> is still greatly limited, due to the quick combination of photo generated electron and hole pairs. Therefore, coupling AgFeO<sub>2</sub> with different semiconductors of matched band position would be an ideal way to modify of photocatalysts methods [9,10]. For example, Tang et al. reported the photocatalytic performance of AgFeO<sub>2</sub>/g-C<sub>3</sub>N<sub>4</sub> with an enhanced acid red G photocatalysis activity [11].

Recently, CdS has attracted great interest for its narrow bandgap and high CB position. CdS can be a prime candidate for solar energy absorption for its slow reflectance in the visible region. However, the photocatalytic stability of pure CdS is very low, because of photogenerated charge carriers restricts its practical application during the photocatalytic reaction [12-15]. Many

---

\*Corresponding author: songzheszh@126.com

CdS based heterojunction photocatalysts have been prepared via different methods, including CuS-CdS/TiO<sub>2</sub> [16], C<sub>60</sub>/CdS [17], CdS/MnWO<sub>4</sub> [18], C/CdS [19], which exhibited excellent photocatalytic performance. To the best of our knowledge, there is no report on the heterojunction of CdS/AgFeO<sub>2</sub>. If CdS particles are coupled with AgFeO<sub>2</sub>, it is possible to improve the efficiency as compared with AgFeO<sub>2</sub> alone, leading to high photocatalytic performance.

Herein, we report a facile method for the synthesis of CdS/AgFeO<sub>2</sub> heterojunction, and we evaluate the photocatalytic activity of prepared different molar ratios of CdS/AgFeO<sub>2</sub> samples under visible light irradiation. Our results showed that the as-prepared CdS/AgFeO<sub>2</sub> heterojunction has superior photocatalytic efficiency in decomposing organic pollutants under visible light irradiation.

## 2. Experimental

### 2.1 Materials

AgNO<sub>3</sub>, Fe(NO<sub>3</sub>)<sub>3</sub>·9H<sub>2</sub>O, NaOH, Na<sub>2</sub>S and other reagents were obtained from commercial sources. Milli-Q water (resistivity >18.0 MΩ·cm) was used throughout the experiments. All the chemicals used in this work without further purification.

### 2.2 Preparation of AgFeO<sub>2</sub> composite

Pure AgFeO<sub>2</sub> was synthesized via a hydrothermal method as follows: AgNO<sub>3</sub> (0.85g) and Fe(NO<sub>3</sub>)<sub>3</sub>·9H<sub>2</sub>O (2.02g) were dissolved into 75 mL of deionized water under magnetic stirring. As precipitating agent, NaOH (1.50g) was added into the above solution under magnetic stirring for 30 min, thus forming suspension mixture. Then the suspension mixture was transferred into 100 ml Teflon-lined stainless steel reactor and heated to 180°C for 24 h under autogenous pressure. The mixture was allowed to cool to room temperature and the as-prepared precipitate was filtered, washed three times with deionized water and dried in an oven at 60°C for 12 h.

### 2.3 Preparation of different molar ratio of CdS/AFO sample

Preparation of CdS/ AgFeO<sub>2</sub> (mole ratio is 1:1 of CdS to AgFeO<sub>2</sub>) sample: AgFeO<sub>2</sub> (0.392g) and Cd(Ac)<sub>2</sub> (0.266g) were dispersed in 50 mL of deionized water by vigorously stirring for 30 min, thus forming suspension mixture A. Na<sub>2</sub>S·9H<sub>2</sub>O (0.24g) was added in 10 ml deionized water formed solution B, and the solution B was added dropwise in mixture A under vigorously stirring for 20 min. The resulting precipitates were collected and washed with deionized water and dried at 60°C for 12 h. The CdS/AFO (mole ratio is 1:1 of CdS to AgFeO<sub>2</sub>) sample was marked as CdS/AFO-1:1. Different CdS/AFO samples were obtained by adjusting the mole ratio of Cd(Ac)<sub>2</sub> and Na<sub>2</sub>S, and the as-synthesized CdS/AFO photocatalysts were marked as CdS/AFO-0.5:1, CdS/AFO-1:1, CdS/AFO-2:1, CdS/AFO-3:1 and CdS/AFO-4:1, respectively. (AFO means AgFeO<sub>2</sub>).

### 2.4 Characterization of catalytic

The crystalline structure of composites was characterized by X-ray diffraction (2θ ranged from 10° to 80°). The morphological features of the composites were characterized by using a scanning electron microscope (SEM). The surface composition of the composites was ascertained

by using the Energy Dispersive Spectroscopy (EDS), which connected with SEM. The Photoluminescence spectroscopy (PL) spectra were collected on fluorescence spectrophotometer (HITACHI F-7000).

### 2.5 Photocatalytic experiments

The photocatalytic activity of the samples was evaluated by degradation of Congo Red (CR) solution under the radiation of a 300 W Xe lamp. Typically, 0.05 g of the sample was added into 100 ml of CR solution (10 mg/L) in dark for 40 min to achieve absorption equilibrium between dye and photocatalyst. Then about 3mL of suspension was withdrawn and collected by centrifuging at 5000 rpm for 10 min. The top clear solution of CR was analyzed by a UV-vis spectrophotometer (UV-1600) at wavelength of 495 nm.

## 3. Results and discussion

### 3.1 Characterization

The phase of obtained AgFeO<sub>2</sub> sample was analyzed by X-ray diffraction (XRD), which are showed in Fig. 1a). The characteristic diffraction peaks for pure AgFeO<sub>2</sub> sample are situated at 2θ (scattering angle) about 14.3°, 28.8°, 34.4°, 35.4°, 39.3°, 43.8°, 52.4°, 59.6°, 61.0°, 68.8° and 72.5° assigning to the lattice planes of the (003), (006), (101), (102), (104), (009), (108), (012), (110), (116) and (202), respectively. These observed peaks match well with standard spectrum AgFeO<sub>2</sub> (PDF 21-1081) which corroborates the samples synthesized. Furthermore, there no characteristic diffraction peaks could be attributed to foreign matters or other phases, the result suggests the high purity of AgFeO<sub>2</sub>.

On the other hand, as shown in Fig. 1b), the principal peaks in the patterns could have an acceptable agreement with the standard spectrum of hexagonal CdS (PDF no. 75-1546). The characteristic diffraction peaks located at 2θ values of 26.5°, 30.7°, 44.0°, 52.1°, 54.6°, 63.9°, 70.5°, 72.6°, 80.8° and 86.9° can be assigned to the (111), (200), (220), (311), (222), (400), (331), (420), (422) and (511) lattice planes of CdS structure, respectively. Besides, while increasing the mole ratio to CdS/AFO, the peaks at 2θ = 26.5 arise and get evident increasingly. The result indicates that a preferential aspect along the (111) plane of the CdS (PDF No.75-1546) is generated. Moreover, that also could be used to demonstrate that CdS have been deposited on AgFeO<sub>2</sub> laminar composite with success.

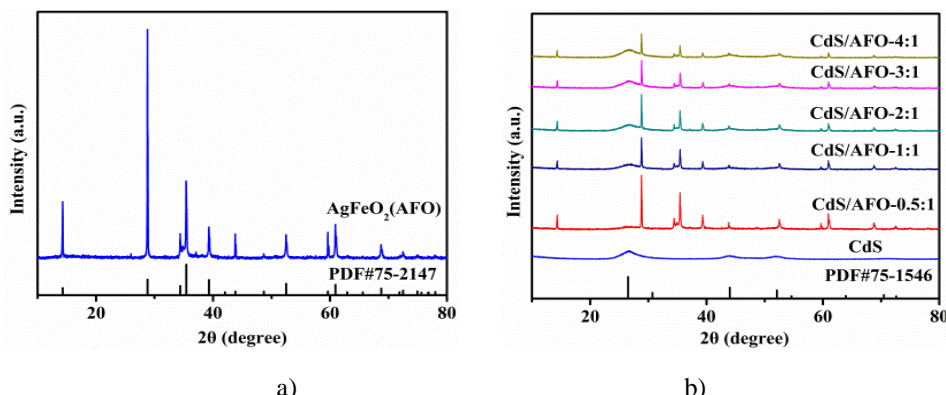


Fig.1 XRD patterns of a) pure AgFeO<sub>2</sub>, b) CdS and CdS/AFO composites

### 3.2 Morphology analysis

To reveal the morphology of pure CdS, AgFeO<sub>2</sub> and CdS/AFO, they are analyzed by SEM analysis as shown in Fig. 2. Fig. 2 (a) displays the evidence of synthesized AgFeO<sub>2</sub> material, which shows 2D nanosheets-type morphology.

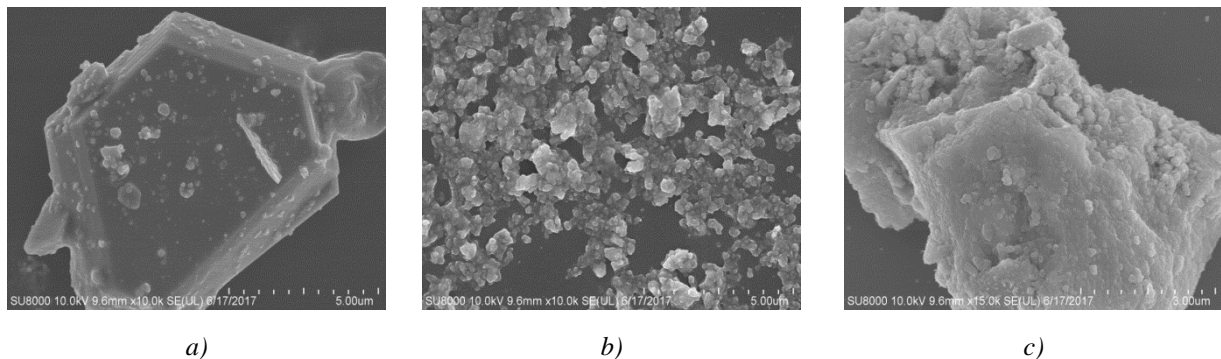
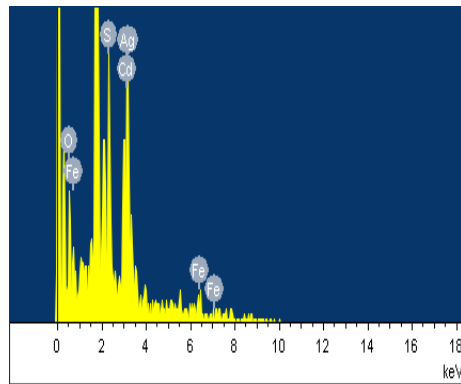


Fig. 2 SEM imagines of a) AgFeO<sub>2</sub>, b) CdS and c) CdS/AFO-2:1

The hydrothermally grown AgFeO<sub>2</sub> nanosheets arrays are about 13  $\mu\text{m}$  with the smooth lateral surface, and the sheet diameter size ranging from 50 nm to 150 nm. After chemical bath deposition of CdS material, the sheet surface of AgFeO<sub>2</sub> arrays is uniformly covered with CdS particles entirely from the bottom to the top end of the array (Fig.2(b), Fig.2(c)). The perfect coverage on the large sheets is ascribed to the optimization of the process which has the high nucleation density and uniformity on AgFeO<sub>2</sub> material, and it accounts for the high efficiency degradation of CR.

### 3.3 EDS analysis

As can be seen in Fig. 3, the elemental composition was determined by EDS mapping, which were detected on the CdS/AFO-2:1 composites sample. It illustrates independent peaks for silver (Ag), oxygen (O), cadmium (Cd), sulfur (S) and iron (Fe) species, which suggested AgFeO<sub>2</sub> and CdS were obtained successfully. Furthermore, in order to investigate elements dispersion, EDS dot-mapping micrographs together with SEM image of region of study were shown in Fig.4. Compared with the SEM image, it has been confirmed that the Ag, Fe and O elements, which are the elements from AgFeO<sub>2</sub>, are exclusively distributed in the centre area of the imaged composites sample. On the other hand, the S element is mainly detected in the surface area of the composites sample, which clearly implies that the CdS covered the CdS/AFO-2:1 nanocomposite as a layer.



*Fig.3 The EDS patterns of CdS/AFO-2:1 composite*

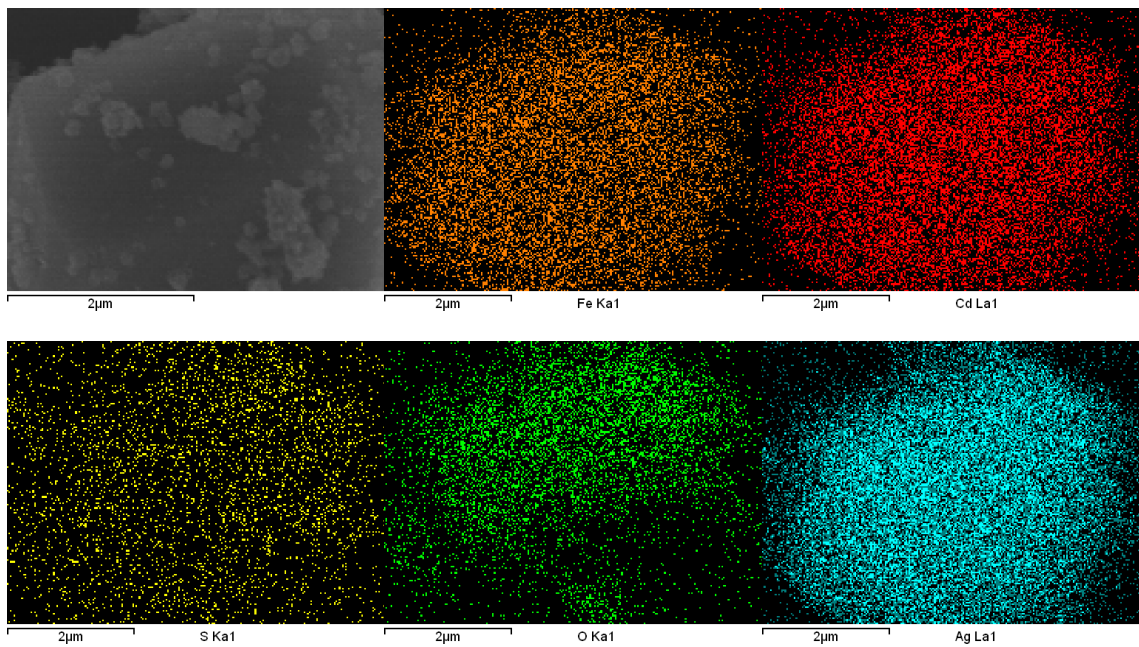


*Fig.4 EDS dot mapping analysis of synthesized nanostructured CdS/AFO-2:1 photocatalyst*

### 3.4 PL spectra

Fig. 5 shows the PL emission spectra of the as-prepared materials under excitation at 405 nm. As seen, the PL emission intensity of the CdS/AFO-0.5:1, CdS/AFO-1:1, CdS/AFO-2:1, CdS/AFO-3:1 and CdS/AFO-4:1 are lower than that of pure CdS and pure Ag<sub>3</sub>FeO<sub>4</sub> nanoparticles, indicating that the introduction of CdS nanoparticles can improve the charge separation. It is evidently observed that the PL intensity from the CdS/AFO-2:1 nanocomposite is significantly smaller as compared to that of the as-prepared materials. This result indicates that incorporation of CdS nanoparticles on the surface of Ag<sub>3</sub>FeO<sub>4</sub> nanoparticles providing trapping sites of electrons in the band gap of Ag<sub>3</sub>FeO<sub>4</sub>.

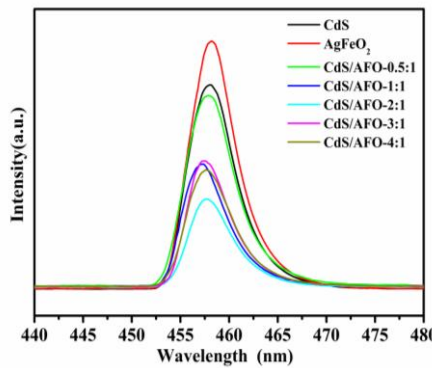


*Fig. 5 PL spectra of pure CdS, pure AgFeO<sub>2</sub> and CdS/AFO composites*

### 3.5 Photocatalytic activity of photocatalyst

The photocatalytic activities of AgFeO<sub>2</sub>, CdS, and CdS/AFO heterojunction were assessed by degradation of CR solution (10 mg/L) under visible light irradiation, as shown in Fig.6. Over the pure pure AgFeO<sub>2</sub>, about 20.43% of CR was removed for 60 min under the condition of visible light. For CdS decorated AgFeO<sub>2</sub> nanocomposites, it can be observed that the photocatalytic performance obviously increased with the incensement of CdS content. Compared to other synthesized CdS/AFO nanocomposites, CdS/AFO-2:1 sample indicates the highest photocatalytic efficiency for CR degradation, with an efficiency of 74.8% over the same time duration.

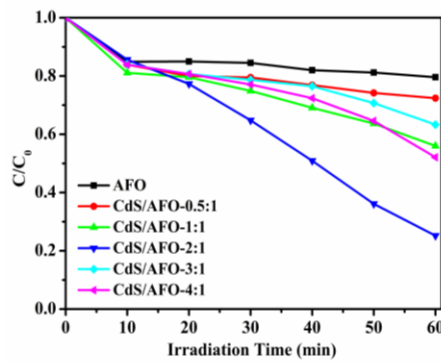


*Fig. 6. Photocatalytic degradation of CR with different as-prepared photocatalyst.*

For the consideration of photocatalytic mechanism, the degradation of CR over AgFeO<sub>2</sub>, CdS, and CdS/AFO was performed to study the optical absorptions in the UV-vis region photocatalytic property of CdS/AFO heterojunction. As a result of the photocatalytic activities, the consequences were ascribed to the synergistic effects of visible light absorption and efficient heterojunction system of CdS/AgFeO<sub>2</sub>. The cause of these enhancements can be summarized as follows: on the one hand, the band position of AgFeO<sub>2</sub> and CdS is matched for forming a suitable heterojunction, which created an effective transfer of the photogenerated charges the synergistic effect; on the other hand, CdS is also a sensitizer with the incensement of optical absorptions; in addition, after CdS nanoparticles decorated the AgFeO<sub>2</sub> nanosheets, the peculiar surface area of AgFeO<sub>2</sub> also generated, and that is conducive to create plentiful active reactors.

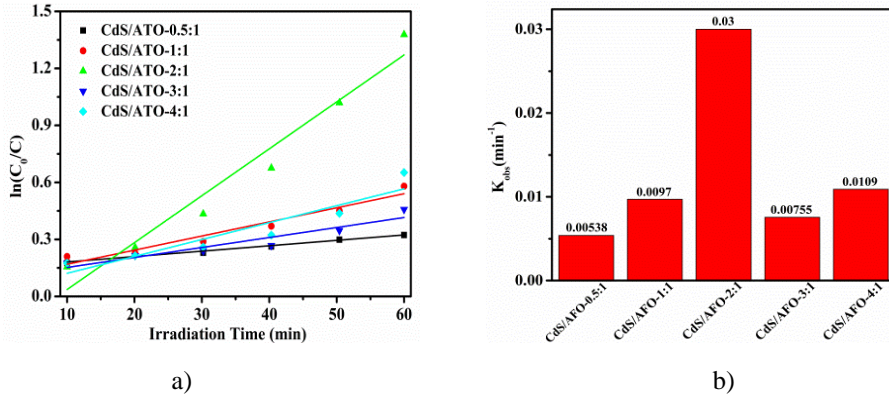


Fig.7. a) Photocatalytic kinetics of each process in degrading CR, and b) first-order rate constant of different as-obtained samples

Besides, in order to investigate the kinetics character of the process of photocatalysis, the reaction kinetics of the degradation is expressed by applying a first-order model as follow Eq. (1) [20,21]:

$$\ln(C_0/C) = K_{obs}t \quad (1)$$

where  $C_0$  and  $C$  are the concentrations of CR in the degradation at times 0 and  $t$ , respectively.  $K_{obs}$  denoted the apparent first-order rate constant. The linear relationship and degradation rate constant are shown in Fig. 7 (a) and Fig. 7 (b), respectively. As illustrated in Fig. 7 (a), the slope for process with CdS/AFO-2:1 was larger than the other CdS/AFO. From Fig. 7 (b), we can see that the rate constant of CdS/AgFeO<sub>2</sub>-2:1 was the maximal of 0.03 min<sup>-1</sup>, which demonstrated the photocatalytic efficiency of CdS/AFO-2:1 was the best in the as-prepared samples.

### 3.6 Reaction mechanism

#### 3.6.1 Effects of reactive species

A sequence of active species trapping tests for CR photodegradation process over the CdS/AFO-2:1 catalyst was accomplished to analyse the dominant reactive species working (Fig.8(a), Fig.8(b)).

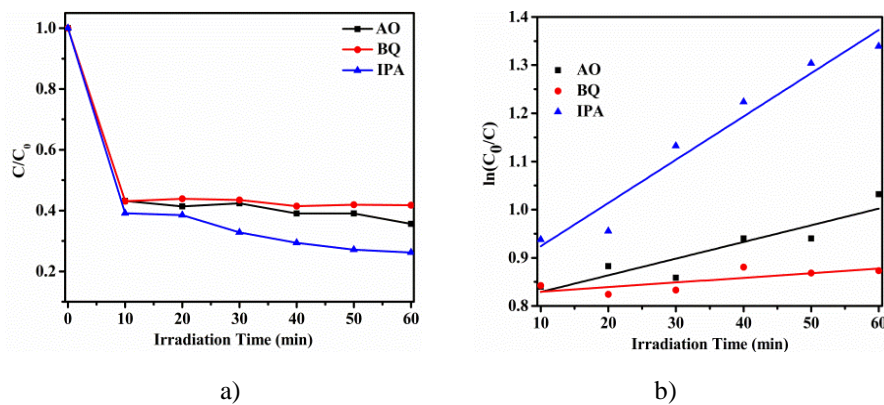
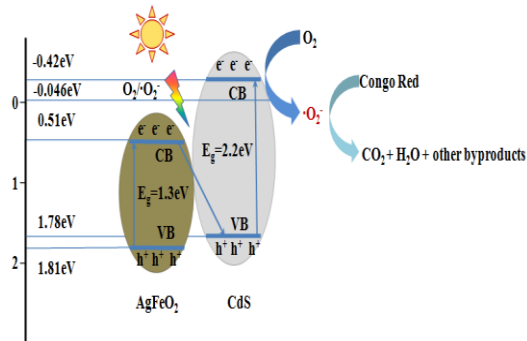
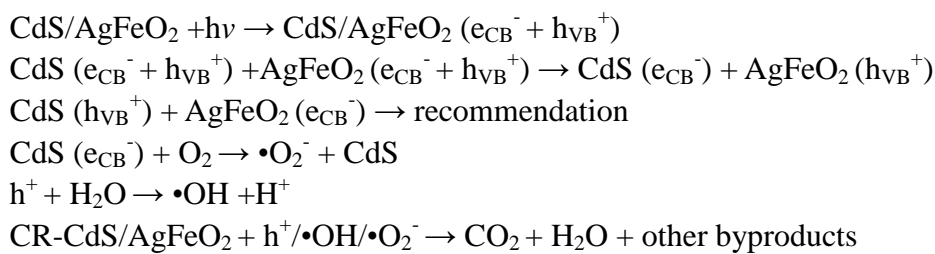


Fig. 8 (a) Photocatalytic degradation with different scavengers, (b) Photocatalytic kinetics of each process with different scavengers

During the CR photodegradation test, superoxide radical ( $\bullet\text{O}_2^-$ ), hydroxyl radical ( $\bullet\text{OH}$ ) and hole ( $\text{h}^+$ ) could be scavenged via adding 1mM benzoquinone (BQ), isopropanol (IPA) and ammonium oxalate (AO). After the IPA took part in the system, the photodegradation rates of CR dropped to 73.7%. Nevertheless, when BQ and AO participated in the degradation process, the photocatalytic potency is virtually restraining, and the degradation rate of CR only dropped to 34%, and 41% under the identical condition respectively. On the basis of the above analyze testing data, it could be certainly concluded that superoxide radical ( $\bullet\text{O}_2^-$ ) and hole ( $\text{h}^+$ ) played important roles toward CR degradation.

### 3.6.2 Photocatalytic activity enhancement mechanism of CdS/AFO composites

Based on the above experimental result, a possible mechanism of CdS/AFO hybrids was proposed for the degradation of CR dyes under solar light irradiation (Scheme 1). The possible electrons transfer process might be described as follows:



Scheme 1. The schematic possible mechanism of degradation of CR by CdS/AFO-2:1 heterostructure

At first, under visible light, AgFeO<sub>2</sub> and CdS can be excited to form the photoexcited holes ( $\text{h}^+$ ) and electrons ( $\text{e}^-$ ) in their VB and CB, respectively. Because the CB edge potential of CdS (-0.42 eV) is more negative than the reduction potential of  $\text{O}_2/\bullet\text{O}_2^-$  (-0.046 eV) [22], the photoelectrons ( $\text{e}^-$ ) photoproduced in AgFeO<sub>2</sub> were transferred across the interface of the CdS/AFO hybrids to the surface of CdS, which consequently reduces the recombination of the photoexcited carriers greatly. The enriched electrons on the surface of CdS could be trapped by molecular oxygen in solution to form  $\bullet\text{O}_2^-$ . Subsequently, the CR molecules were attacked by the generated the free radicals ( $\bullet\text{O}_2^-$ , etc.), leading to the decolorization and opening ring reactions. Finally, the active species oxidized the dye molecules to the degradation products ( $\text{CO}_2$ ,  $\text{H}_2\text{O}$ , other byproducts.).

#### 4. Conclusions

The CdS/AFO hybrids were grown by co-precipitation on the surfaces of hydrothermally prepared AgFeO<sub>2</sub> to form the heterojunction nanocomposite. The as-prepared CdS/AFO composites show much higher photocatalytic activities for the degradation of CR than the pure AgFeO<sub>2</sub> due to the matched band structure of two components and more effective charge transportation and separations. The suggested catalyst provides an effective and environmentally friendly catalyst with relatively good activity. Thus, CdS/AFO composites are very promising in the treatment of organic pollutants in wastewater.

#### Acknowledgments

This work was financially supported by Natural Science Foundation of Changchun Normal University ([2010]009), and the Natural Science Project Foundation of Education Department of Jilin Province of China (No.2015358), and the Natural Science Foundation of Changchun Normal University(No. 201203).

#### References

- [1] X. B. Chen, S. Shen, L. Guo, S. S. Mao, *Chen. Rev.* **110**, 6503 (2010).
- [2] F. Li, Y. Dong, W. Kang, B. Cheng, G. Cui, *Appl. Surf. Sci.* **404**, 206 (2017).
- [3] H. Tong, S. X. Quyang, Y. P. Bi, N. Umezawa, I. Oshikiri, J. H. Ye, *Adv. Mater.*, **24**, 229 (2014).
- [4] X. F. Yang, J. L. Qin, Y. Li, H. Tang, *J. Hazard. Mater.* **261**, 342 (2013).
- [5] J. D. Li, W. Fang, C. L. Yu, W. Q. Zhou, L. H. Zhu, Y. Xie, *Appl. Surf. Sci.* **358**, 46 (2015).
- [6] X. F. Wu, L. L. Wen, K. L. Lu, K. J. Deng, D. G. Tang, H. P. Ye, D. Y. Du, S. N. Liu, M. Li, *App. Surf. Sci.* **358**, 130 (2015).
- [7] A. Vasiliev, O. Volkova, I. Presniakov, A. Baranov, G. Demazeau, J. M. Broto, M. Millot, N. Leps, R. Klingeler, B. Buchner, M. B. Stone, A. Zheludev, *J. Phys. Condens. Matter.* **22**, 1 (2010)
- [8] W. C. Sheets, E. S. Stampler, M. I. Bertoni, M. Sasaki, T. J. Marks, T. O. Mason, K. R. Poeppelmeier, *Inorg. Chem.* **47**, 2696 (2008).
- [9] D. D. Tang, G. K. Zhang, *Ultrason. Sonochem.* **37**, 208 (2017)
- [10] S. M. Hosseini, H. H. Monfared, V. Abbasi, M. R. Khoshroo, *Inorg. Chem. Commun.* **67**, 72 (2016).
- [11] D. D. Tang, G. K. Zhang, *Appl. Surf. Sci.* **391**, 415 (2017).
- [12] H. Yang, Z. L. Jin, K. Fan, D. D. Liu, G. X. Lu, *Superlattice. Microst.* **111**, 687 (2017).
- [13] K. Veerathangam, M. S. Pandian, P. Ramasamy, *Mater. Res. Bull.* **94**, 371 (2017).
- [14] S. Mathew, B. Samuel, A. Mujeeb, M. Kailasnath, V. P. N. Nampoori, C. P. Girijavallabhan, *Opt. Mater.* **72**, 673 (2017).
- [15] M. E. Khan, M. M. Khan, M. H. Cho, *J. Colloid. Interf. Sci.* **482**, 221 (2016).
- [16] M. Maleki, M. Haghghi, *J. Mol. Catal. A-Chem.* **424**, 283 (2016).
- [17] Q. Cai, Z. F. Hu, Q. Zhang, B. Y. Li, Z. R. Shen, *Appl. Surf. Sci.* **403**, 151 (2017).
- [18] X. Yan, K. L. Liu, W. D. Shi, *Colloid. Surface. A* **502**, 138 (2017).

- [19] F. X. Wang, L. Liang, K. L. Chen, J. M. Sun, *J. Mol. Catal. A-Chem.* **425**, 76 (2016).
- [20] G. Elango, S. M. Roopan, *J. Photochem. photobio.* **155**, 34 (2016).
- [21] A. Phuruangrat, A. Maneechote, P. Dumrongjithanath, N. Ekthammathat, S. Thongtem, T. Thongtem, *Mater. Lett.* **159**, 289 (2015).
- [22] Y. N. Lin, R. X. Wang, Z. K. Yang, H. Du, Y. F. Jiang, C. C. Shen, K. Liang, A. W. Xu, *Chin. J. Catal.* **36**, 2135 (2015).